





# Amplification of GaSb-Based Diode Lasers in an Erbium-Doped Fluoride Fibre Amplifier

Nikolai B. Chichkov , Amit Yadav , Franck Joulain, Solenn Cozic, Semyon V. Smirnov, Leon Shterengas , Julian Scheuermann, Robert Weih, Johannes Koeth, Sven Höfling, Ulf Hinze, Samuel Poulain, and Edik U. Rafailov , *Senior Member, IEEE*

**Abstract**—Building upon recent advances in GaSb-based diode lasers and Er-doped fluoride fibre technologies, this article demonstrates for the first time the fibre-based amplification of mid-infrared diode lasers in the wavelength range around 2.78  $\mu\text{m}$ . The laser setup consists of a GaSb-based diode laser and a single-stage Er-doped fibre amplifier. Amplification is investigated for continuous wave (CW) and ns-pulsed input signals, generated by gain-modulation of the GaSb-based seed lasers. The experimental results include the demonstration of output powers up to 0.9 W, pulse durations as short as 20 ns, and pulse repetition rates up to 1 MHz. Additionally, the amplification of commercial and custom-made GaSb-based seed lasers is compared and the impact of different fibre end-cap materials on laser performance is analysed.

**Index Terms**—Erbium, fibre laser, fluoride fibre, GaSb diode laser, mid-infrared, nanosecond, semiconductor laser, ZBLAN.

Manuscript received 22 November 2022; revised 9 January 2023; accepted 15 January 2023. Date of publication 19 January 2023; date of current version 2 February 2023. The data that support the findings of this study are available from the corresponding author upon reasonable request. This work was supported in part by Marie Skłodowska-Curie through European Union's Horizon 2020 Research and Innovation Programme under Grant 843801 and in part by Engineering and Physical Sciences Research Council (EPSRC) under Grant EP/R024898/1. (*Corresponding author: Nikolai B. Chichkov.*)

Nikolai B. Chichkov is with the Institute of Quantum Optics, Leibniz University Hannover, 30167 Hannover, Germany, and also with the Aston Institute of Photonic Technologies, Aston University, Birmingham B4 7ET, U.K. (e-mail: n.chichkov@iqo.uni-hannover.de).

Amit Yadav, Semyon V. Smirnov, and Edik U. Rafailov are with the Aston Institute of Photonic Technologies, Aston University, Birmingham B4 7ET, U.K. (e-mail: a.yadav1@aston.ac.uk; s.smirnov@itmo.ru; e.rafailov@aston.ac.uk).

Franck Joulain, Solenn Cozic, and Samuel Poulain are with the Le Verre Fluoré, Campus KerLann, F-35170 Bruz, France (e-mail: franck.joulain@leverrefluore.eu; solenn.cozic@leverrefluore.eu; samuel.poulain@leverrefluore.eu).

Leon Shterengas is with the Department of Electrical and Computer Engineering, Stony Brook University, Stony Brook 11794 USA (e-mail: leon.shterengas@stonybrook.edu).

Julian Scheuermann and Johannes Koeth are with the Nanoplus GmbH, 97218 Gerbrunn, Germany (e-mail: julian.scheuermann@nanoplus.com; koeth@nanoplus.com).

Robert Weih is with the Nanoplus GmbH, 97218 Gerbrunn, Germany, and also with the Technische Physik, Physikalisches Institut und Wilhelm Conrad Röntgen-Research Center for Complex Material Systems, University of Würzburg, 97074 Würzburg, Germany (e-mail: robert.weih@nanoplus.com).

Sven Höfling is with the Technische Physik, Physikalisches Institut und Wilhelm Conrad Röntgen-Research Center for Complex Material Systems, University of Würzburg, 97074 Würzburg, Germany (e-mail: sven.hoefling@physik.uni-wuerzburg.de).

Ulf Hinze is with the Institute of Quantum Optics, Leibniz University Hannover, 30167 Hannover, Germany, and also with the Laser nanoFab GmbH, 30419 Hannover, Germany (e-mail: u.hinze@lasernanofab.de).

Digital Object Identifier 10.1109/JPHOT.2023.3238078

## I. INTRODUCTION

A WIDELY used laser configuration, with a variety of applications in science and industry, is the amplification of electrically-pumped semiconductor lasers in high-power, rare-earth-doped fibre amplifiers. Diode lasers are highly-compact, efficient, and mass-producible laser devices, which provide direct electrical-control and enable the translation of high-frequency electrical signals into intensity modulated laser output [1]. Depending on device design (e.g. distributed feedback, external-cavity, etc.), diode lasers are able to provide highly stable, narrow linewidth laser operation and broad wavelength tunability. Rare-earth doped fibre amplifiers are used for efficient power-scaling of the diode laser output, enabling amplified output powers of several 100 W in combination with diffraction-limited beam profiles [2], [3], [4]. Optical fibre amplifiers benefit from efficient cooling possibilities, high optical-to-optical conversion efficiencies, and straightforward control of output beam parameters through the choice of fibre dimensions.

Electrically-modulated diode lasers and signal amplification in Er-doped fibres, operating around 1550 nm, are the technical foundation of modern telecommunication systems and networks [5]. Yb-based fibre amplifiers and ns-pulsed GaAs-based diode lasers with emission wavelengths around 1040 nm are widely used for applications in laser material processing [3], [4]. These applications include the cutting and drilling of metal parts, marking and labelling of components, and surface structuring of plastics and metals.

In the last two decades, there have been increasing efforts to extend the wavelength range of fibre-amplifiers and diode lasers into the MIR, motivated by new applications in spectroscopy [6], [7] and material processing [8], [9], [10], [11]. The main interest for material processing applications is the use of MIR laser radiation for the processing of materials, which have low absorption coefficients or are transparent in the near-infrared (NIR). This includes various polymers and organic materials with C-H molecular bonds which have absorption peaks around 3.4  $\mu\text{m}$  [8], glass materials with O-H contaminants which exhibit strong absorption near 2.7  $\mu\text{m}$  [12], and biological materials with an absorption maximum at 2.9  $\mu\text{m}$  from the O-H molecular bond in liquid water [13].

Major advances have been achieved in the development of GaSb-based diode lasers, which are now able to provide laser emission over a broad wavelength range from 1.9  $\mu\text{m}$  up to 3.2  $\mu\text{m}$  [14], [15]. The output powers of GaSb-based diode lasers

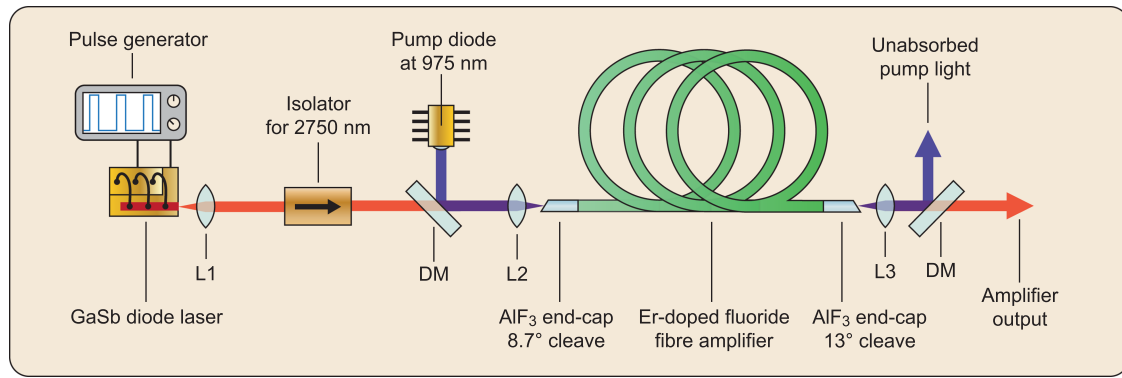


Fig. 1. Laser setup consisting of GaSb-based diode laser and a single stage Er-doped fluoride fibre amplifier. L1: BD-2 lens,  $f = 4$  mm; L2: CaF<sub>2</sub> lens,  $f = 20$  mm; L3: CaF<sub>2</sub> lens,  $f = 25$  mm; DM: Dichroic mirror HT at 2780 nm and HR at 975 nm.

at room-temperature have increased substantially, reaching up to 20 mW for single-mode devices with emission wavelengths around  $3.2 \mu\text{m}$ . At the same time significant improvements in the performance of rare-earth doped fluoride fibre lasers have been attained [16], [17]. Fluoride-based fibres are used to replace silica-based counter-parts for applications in the MIR. Whereas, conventional silica fibres suffer from strong absorption at wavelengths above  $2.2 \mu\text{m}$ —preventing optical waveguiding and laser amplification at longer wavelengths—fluoride fibres exhibit low transmission losses in the entire MIR wavelength range. Rare-earth doping of fluoride fibres has enabled the development of MIR fibre lasers and amplifiers at wavelengths from  $2.3 \mu\text{m}$  up to  $4.0 \mu\text{m}$  [16]. Output powers of up to 40 W have been achieved from Er-doped fluoride fibre lasers, operating at wavelengths around  $2.8 \mu\text{m}$  [18]. Several fluoride fibre amplifier systems have been demonstrated, including the amplification of femtosecond pulses from a mode-locked fibre laser [19], picosecond pulses from optical parametric generator systems [20], [21], [22], and nanosecond pulses from optical parametric oscillators [23], [24], [25].

In this article, we combine the recent developments in GaSb-based diode lasers and fluoride fibre amplifiers to demonstrate—for the first time to the best of our knowledge—the amplification of GaSb-based diode lasers in an Er-doped single-mode fluoride fibre amplifier. In the following, we present the amplification of CW and ns-pulsed laser signals, compare two different seed lasers, and analyse the influence of fluoride fibre end-caps on the laser output. The second and third section of the article introduce the experimental setup and present the amplification of a GaSb-based cascaded type-I quantum well (CQW) diode laser. This seed laser provided output powers of more than 20 mW in CW operation, which enabled efficient optical saturation of the fibre amplifier. In the fourth section, the CQW diode laser is replaced by a commercially available GaSb-based quantum-well (QW) laser (provided by nanoplus, Nanosystems and Technologies GmbH). This seed laser provided significantly lower average powers, which resulted in a decline of the optical efficiency of the fibre amplifier system. Experiments with this seed laser were performed to investigate the reproducibility of the obtained results. Finally, in the fifth section, we compare the impact of different fibre end-caps on the laser output.

## II. EXPERIMENTAL SETUP

The experimental setup is illustrated in Fig. 1. The laser system consisted of a seed laser part and a single-stage fibre amplifier. The seed laser was a custom-made type-I CQW GaSb-based diode laser with a Fabry-Pérot cavity, designed and fabricated at the Stony Brook University and similar in terms of waveguide and layer structure to the devices reported in reference [14]. The CQW laser design included a  $7 \mu\text{m}$  wide narrow ridge waveguide, which resulted in spatial single-mode operation with an elliptical output beam profile.

The seed laser was mounted epi-side up on a standard C-mount and temperature stabilised on a copper heat sink at temperatures of  $20^\circ\text{C}$  and  $25^\circ\text{C}$  for CW and ns-pulsed operation, respectively. The laser was connected to a DC current driver (Thorlabs ITC4000) for continuous wave operation and to a pulse generator (Agilent 8114 A) for ns-pulsed operation. The CQW laser output was collimated with an AR-coated aspheric lens (BD-2,  $f = 4$  mm) and coupled with an uncoated, plano-convex CaF<sub>2</sub> lens ( $f = 20$  mm) into the fibre section. A tunable isolator set to 2750 nm (Thorlabs I2700Y4) was used to protect the CQW laser from back-reflections. A total coupling efficiency of 16% was achieved, including losses at intermediate optical components and 40% transmission losses at the optical isolator. The low coupling efficiency is a consequence of the mismatch between the elliptical beam profile of the CQW laser and the fibre mode. Improvement of coupling efficiency in future setups can be achieved by the use of cylindrical CaF<sub>2</sub> lenses to increase the mode overlap.

The fibre amplifier consisted of a 2.2 m long section of commercial Er-doped double-clad fluoride fibre, provided by Le Verre Fluoré. The fibre had a doping concentration of 7 mol% and a D-shaped pump cladding with a diameter of  $260 \mu\text{m}$  and numerical aperture (NA) of 0.46. The fibre core had a core diameter of  $15.5 \mu\text{m}$  with a NA of 0.125, corresponding to a cut-off wavelength of  $2.5 \mu\text{m}$  for single-mode operation. The same fibre model was used in previous publications for the demonstration of fibre lasers and amplifiers at wavelengths around  $2.8 \mu\text{m}$  [18], [20], [23]. Two core-less fluoroaluminate (AlF<sub>3</sub>) end-caps were spliced at the ends of the fibre section to prevent fibre damages and degradation from O-H diffusion [26], [27]. Both end-caps

were angle-cleaved to suppress back-reflections and parasitic lasing. The end-cap on the input end of the fibre had a length of 0.8 mm and a cleave angle of  $9^\circ$ , while the output end-cap had a length of 0.7 mm and a cleave angle of  $13^\circ$ . Both fibre ends were placed into copper V-grooves with the fibre tips protruding by about 1 cm.

The fibre section was pumped in co-propagating direction by a multimode pump diode with an emission wavelength of 975 nm and a maximum pump power of 10.1 W. The pump light was delivered in a multimode silica fibre with a core diameter of  $107\ \mu\text{m}$  and NA of 0.22, collimated with an AR-coated lens (focal length  $f = 20\ \text{mm}$ ), and coupled into the input end of the fibre section through the same  $\text{CaF}_2$  lens that was used for the seed laser coupling. A custom-made dichroic mirror (transmission  $> 97\%$  at 2700–3200 nm, reflection  $> 99.5\%$  at 975 nm) was used to combine the seed and pump laser beams. A second dichroic mirror was placed at the amplifier output to remove the unabsorbed pump light. The co-propagating pump configuration was chosen to reduce thermal effects and heating in the output fibre facet [27].

The amplified laser spectra were characterised with a setup consisting of a Horiba iHR320 monochromator with a 300 grooves/mm diffraction grating, a liquid nitrogen cooled InSb-detector, and a lock-in amplifier. The amplified laser spectra were recorded with a wavelength increment of 0.05 nm and a sub-0.2 nm resolution—calculated from the nominal monochromator slit-widths of  $10\ \mu\text{m}$ . The spectra were recorded over the complete wavelength range from 2680–2850 nm with a signal-to-noise ratio of more than 30 dB, to ensure that any parasitic lasing and amplified spontaneous emission (ASE) can be detected if present. The temporal pulse profiles of the amplified ns-pulses were measured with a fast HgCdTe photodetector (Thorlabs, PDAVJ10) with a response bandwidth of 100 MHz (at  $-3\ \text{dB}$ ) and a theoretical rise-time of 3.5 ns.

### III. RESULTS

#### A. Continuous Wave

Amplification was investigated for CW operation and different ns-pulsed regimes. Fig. 2 plots the amplified output power as function of the launched pump power for all operation regimes. The highest output power and slope-efficiency were obtained for CW operation, in which the CQW laser provided a seed power of 22.8 mW. After transmission and coupling-losses, a remaining seed power of 3.7 mW (16%) was injected into the fibre section (measured at the amplifier output). As can be seen from Fig. 2, the amplified output power increased linearly with the applied pump power. An output power of 934 mW was obtained at the maximum pump power of 10.1 W. This value corresponds to an optical efficiency of 9.2%, a slope-efficiency of 9.8%, and an overall optical gain of 16 dB (including coupling-losses).

The seed laser spectrum and amplified output spectra for CW operation are shown in Fig. 3(a). The seed spectrum had a peak wavelength of 2795 nm and a broad pedestal covering the wavelength range from 2760–2800 nm. The 3.3 mm long Fabry-Pérot cavity of the CQW laser resulted in a modulation of the laser spectrum with a period of approximately 0.35 nm. The laser

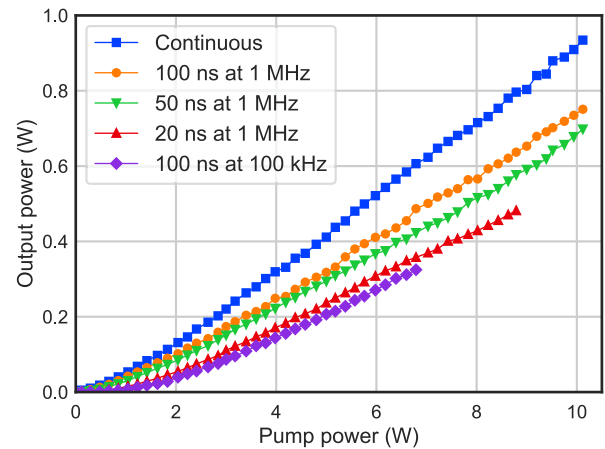


Fig. 2. Amplified output power versus launched pump power for CW and ns-pulsed laser operation.

spectrum remained mostly unchanged after amplification, apart from minor changes due to fibre-coupling and gain-narrowing. The absence of additional spectral components or pedestals in the wavelength range from 2680–2750 nm, demonstrates that ASE was fully suppressed. Parasitic lasing (self-lasing) in the fibre section was also absent—otherwise the onset of parasitic lasing would have led to a pronounced CW spike.

#### B. Pulsed Operation

Gain-modulation of the CQW laser was used to obtain ns-pulses with different pulse durations and repetition rates. This resulted in significantly reduced seed laser powers, proportional to the applied duty-cycle. Pulsed operation was investigated at a repetition rate of 1 MHz for pulse durations of 20 ns, 50 ns, and 100 ns, with CQW seed laser powers (before coupling losses) of 1.4 mW, 3.7 mW, and 7.2 mW, respectively. Additionally, the amplification of 100 ns pulses at a repetition rate of 100 kHz was investigated (1% duty-cycle), corresponding to a seed power of 0.8 mW. At duty-cycles of less than 1%, i.e. at shorter pulse durations or lower repetition rates, the CQW laser power was insufficient to saturate the fibre amplifier, resulting in self-lasing in the fibre section at pump powers above 1 W.

At the repetition of 1 MHz and pulse duration of 100 ns, a maximum amplified output power of 751 mW was obtained (see Fig. 2). This corresponds to an optical efficiency of 7.4%, a slope-efficiency of 8.0%, and an amplifier gain of 20 dB. Reducing the pulse duration to 50 ns resulted in a slightly lower output power of 698 mW, with a slope-efficiency of 7.3% and an amplifier gain of 23 dB. For pulse durations of 20 ns, a maximum output power of 482 mW was obtained at a pump power of 8.8 W. This corresponds to a slope-efficiency of 6.3% and an amplifier gain of 25 dB. The onset of self-lasing at pump powers above 8.8 W prevented further amplification at this pulse duration.

The reduction of the duty-cycle to 1% and operation at 100 kHz with pulse durations of 100 ns further lowered the threshold for self-lasing in the fibre section. The maximum output power (without self-lasing) was obtained at a pump power of 6.8 W. The amplifier generated output pulses with

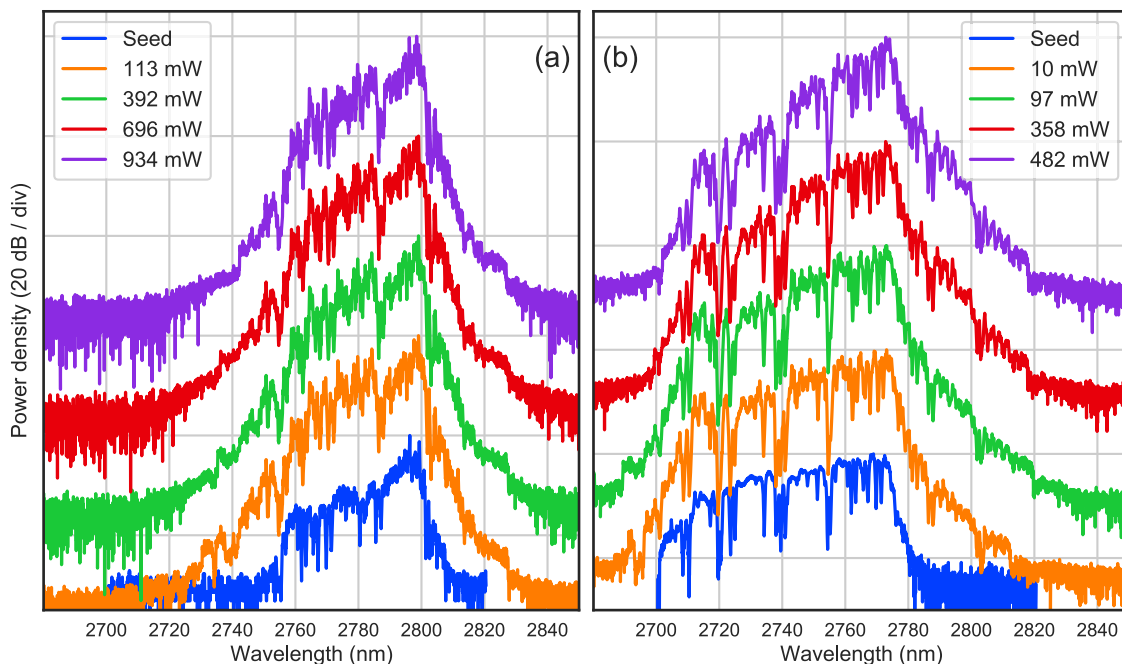


Fig. 3. CQW laser spectrum (blue) and amplified laser spectra at different output powers. (a) Spectra for CW operation. (b) Spectra at 1 MHz with pulse durations of 20 ns.

an average power of 325 mW and pulse energies of  $3.25 \mu\text{J}$ . The slope-efficiency decreased to 5.7% and the amplifier gain reached its maximum value of 26 dB.

The CQW laser spectrum and the spectra of the amplified laser pulses at the repetition rate of 1 MHz with pulse durations of 20 ns are plotted in Fig. 3(b). In comparison to CW operation, ns-pulsed operation resulted in a significantly broader laser spectrum and a shift to shorter wavelengths. The peak emission wavelength was located at 2769 nm and the spectrum covered the wavelength range from 2700 nm to 2780 nm. Amplification resulted in a tilt of the spectral power distribution to the long wavelength part of the spectrum. As can be seen in Fig. 3(b), spectral components near 2770 nm experienced more than 10 dB higher gain than spectral components around 2710 nm. The maximum output power of 482 mW in Fig. 3(b) corresponds to the threshold for parasitic self-lasing in the fibre section. Further increase of the pump power resulted in the build-up of a CW spike at 2784 nm.

Since any potential ASE background is fully overlapped by the broadband spectrum of the amplified laser pulses, it is not possible to estimate the amount of ASE from the output spectrum. To check for potential ASE, the seed laser was blocked and the fibre amplifier was operated without laser input. This resulted in parasitic self-lasing in the fibre section, with a pump power threshold of approximately 1 W. No ASE background was observed during self-lasing operation. This indicates that the single-pass gain threshold for ASE build-up was above the threshold for self-lasing. Thus, self-lasing in the fibre section occurred before any ASE build-up and depleted the amplifier gain, effectively suppressing the generation of ASE. From this, we conclude that no ASE background was present in the amplified laser spectra in Fig. 3(b).

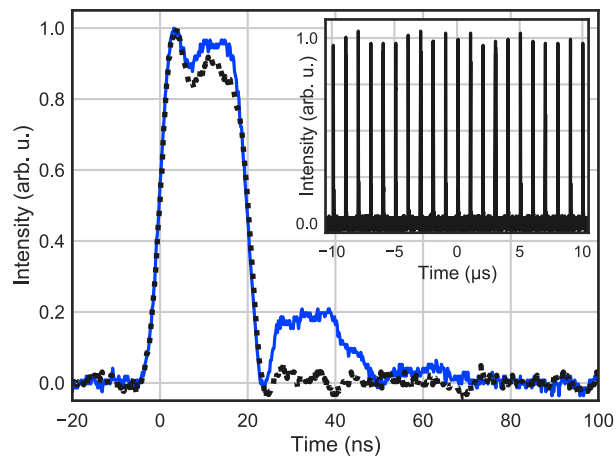


Fig. 4. Oscilloscope trace of the amplified output pulses at a repetition rate of 1 MHz and pulse duration of 20 ns: amplified pulse shape (blue), input pulse shape (black, dotted), and pulse train over a span of  $20 \mu\text{s}$ .

Fig. 4 shows the oscilloscope trace of the amplified output pulses at the repetition rate of 1 MHz and pulse duration of 20 ns. The amplified pulses had an energy of 482 nJ and a peak power of 21 W, calculated by normalisation of the oscilloscope trace. Comparison of the amplified pulse shape with the initial seed pulse, shows the emergence of a trailing satellite pulse after amplification. This pulse contains 15% of the total pulse energy and is located at a delay of 24 ns after the main pulse. The satellite pulse emerges for amplifier gain values above 23 dB, corresponding to a single-pass gain in the fibre section (i.e. without coupling-losses) of 31 dB, and increases in magnitude (relative to the main pulse) at higher gain values. Similar satellite pulses are observable for all other input pulse parameters, except

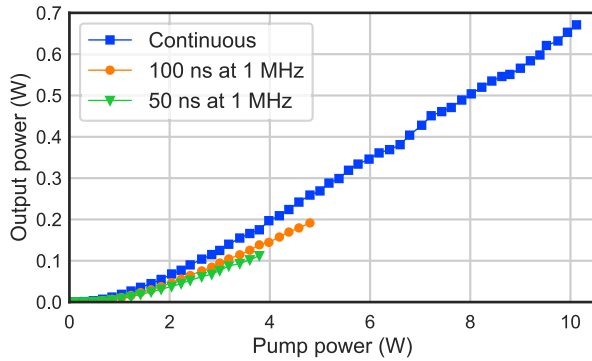


Fig. 5. Amplification of commercial GaSb-based QW laser: output power versus launched pump power for CW and ns-pulsed laser operation.

for 100 ns pulses at 1 MHz for which the amplifier gain remained below 23 dB. The observed delay of the satellite pulse is in good agreement with the time required for the pulse to perform a full round-trip in the fibre section, i.e. propagate from one end of the fibre to the other and back. Thus, the appearance of satellite pulses can be explained by Fresnel back-reflections at the fibre ends, specifically at the splices connecting the fibre section and the  $\text{AlF}_3$  end-caps (see section V).

### C. Laser Stability

The experiments were performed over a period of two and a half weeks. The fibre amplifier was regularly operated over periods of 1–2 hours at the maximum output powers during CW operation and for ns-pulsed regimes. No decline of the laser performance, due to damages or degradation of the  $\text{AlF}_3$  end-caps, was observed. Continuous operation time was limited by dealignment of the fibre-coupling, caused by temperature-induced movement/deformation of the convection cooled fibre-tips, and by thermal drifts in the laser laboratory (not temperature stabilised). Thermal effects were most pronounced at the input fibre facet, where the incident pump light resulted in heat up and movement of the fibre-tip at higher pump powers. For this reason, no systematic laser stability and long term measurements were performed.

## IV. COMMERCIAL SEED LASER

The presented experimental setup relied on the use of a custom-made high-power GaSb-based CQW diode laser to provide sufficient seed power for fibre amplification at low duty-cycles. This type of GaSb-based diode laser is not commercially available and provides significantly higher output powers than typical commercial alternatives at wavelengths near  $2.8 \mu\text{m}$ . To investigate the performance of the presented Er-doped fluoride fibre amplifier with commercially available devices, all experiments were repeated with a commercial Fabry-Pérot GaSb-based QW diode laser, which was obtained from the nanoplus Nanosystems and Technologies GmbH.

The amplified output power versus launched pump power is plotted in Fig. 5 for different operation regimes. The GaSb-QW laser was temperature stabilised at  $20^\circ\text{C}$  and provided a seed

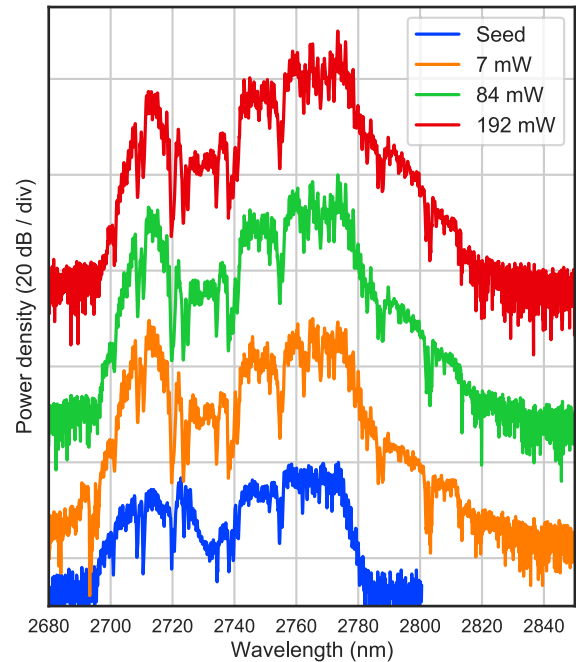


Fig. 6. Amplification of commercial GaSb-based QW laser at 1 MHz with pulse durations of 100 ns: spectrum of seed laser pulses (blue) and spectra of amplified laser pulses at different output powers.

power of 2.7 mW in CW operation. The laser spectrum covered the range of 2765–2785 nm with a peak wavelength of 2782 nm (see Fig. 6). A total coupling efficiency of 11% was obtained, corresponding to a seed power of 0.3 mW injected into the fibre section. Amplification resulted in a maximum output power of 671 mW at a pump power of 10.1 W. An amplifier gain of 24 dB was obtained, with a slope efficiency of 7.3%.

The temperature of the GaSb-QW laser was reduced to  $20^\circ\text{C}$  for ns-pulsed operation. This increased the output power at the expense of shorter emission wavelengths. Pulsed operation was investigated at the repetition rate of 1 MHz with pulse durations of 50 ns and 100 ns, corresponding to seed powers of 0.7 mW and 1.3 mW, respectively. These low seed powers were not sufficient to suppress self-lasing in the fibre section at the maximum pump power—similar to the previous experiments with the CQW diode laser. The onset of self-lasing was observed at pump power thresholds of 3.8 W (at 50 ns) and 4.8 W (at 100 ns). For pulse durations of 100 ns, a maximum output power of 192 mW was obtained, with an amplifier gain of 22 dB and slope efficiency of 4.9%. For 50 ns pulse durations, an amplified output power of 112 mW was obtained, with an amplifier gain of 22 dB and a slope efficiency of 3.8%.

The lower amplifier gain and slope efficiency in comparison to the CQW laser at comparable seed powers can be attributed to the lower fibre-coupling efficiency and to the spectral power distribution of the GaSb-based QW laser. Fig. 6 shows the laser spectrum of the GaSb-based QW laser and the amplified pulse spectra for the pulse duration of 100 ns. The seed spectrum is split into two parts, which together cover the wavelength range from 2700 nm to 2780 nm. The highest amplification is observed for spectral components around 2770 nm. The

peak of the laser spectrum at the maximum output power of 192 mW is located at a wavelength of 2773 nm. The side maximum has a peak wavelength of 2713 nm. The division of the spectral distribution into spectral components around 2710 nm and 2770 nm results in a smaller effective gain and lower seed power near the peak of the amplifier gain around 2780 nm. This reduces the saturation of the fibre amplifier and leads to a lower pump power threshold for self-lasing. It must be noted, however, that the commercial GaSb-based QW laser, used in the experiments, was not optimised for pulsed operation and the measured laser spectrum must not be considered representative. Other commercial GaSb-based devices with different designs may provide spectral distributions, which are better suited for amplification in Er-doped fluoride fibre amplifiers and allow for higher amplifier gain values and output powers.

## V. END-CAP MATERIALS

As described in section III-B, amplification of ns-pulses resulted in the appearance of a trailing satellite pulse at the amplifier output. This pulse was located at a delay of approximately 24 ns after the initial pulse and its relative amplitude increased with higher amplifier gain values. This effect can be explained by Fresnel back-reflections from the  $\text{AlF}_3$  end-caps at both ends of the fibre section, which is consistent with the observed delay and relative amplitude of the satellite pulses.

To further investigate the impact of back-reflections on the amplifier output, three different end-cap configurations were tested. All three configurations used the same type of Er-doped double-clad fibre provided by Le Verre Fluoré. The first configuration consisted of a 2.4 m long fibre section with bare angle-cleaved fibre facets on both ends, with cleave angles of  $7^\circ$  (input) and  $8^\circ$  (output). The second configuration has already been presented in section II and had a 2.2 m long fibre section with angle-cleaved  $\text{AlF}_3$  end-caps at both ends. The third configuration had a 2.4 m long fibre section with a bare angle-cleaved (at  $7^\circ$ ) fibre facet on the input end and a fluorogermanate ( $\text{GeO}_2$ ) end-cap at the output end. The  $\text{GeO}_2$  end-cap was polished at an angle of  $9^\circ$  and had a length  $260 \mu\text{m}$ .

All three configurations were used for the amplification of the GaSb-based CQW laser operating at the repetition rate of 1 MHz with pulse durations of 20 ns. The oscilloscope traces of the amplified laser pulses for each end-cap configuration are shown in Fig. 7. For the configuration with bare fibre ends, an amplified output power of 329 mW was obtained at a pump power of 4.8 W—equivalent to an amplifier gain of 24 dB. No satellite pulses appear in the corresponding oscilloscope trace, confirming the effective suppression of back-reflections by the angle-cleaved fibre facets.

The amplifier setup with  $\text{AlF}_3$  end-caps provided an amplified output power of 357 mW at the pump power of 4.8 W. The oscilloscope trace shows a small trailing satellite pulse with 6.7% of the total pulse energy. Assuming a refractive index of 1.49 for the fibre core and a refractive index of 1.46 for the  $\text{AlF}_3$  end-caps [27], results in a Fresnel reflection with a relative power of  $-39.9$  dB at each end-cap. At the same time a single-pass gain

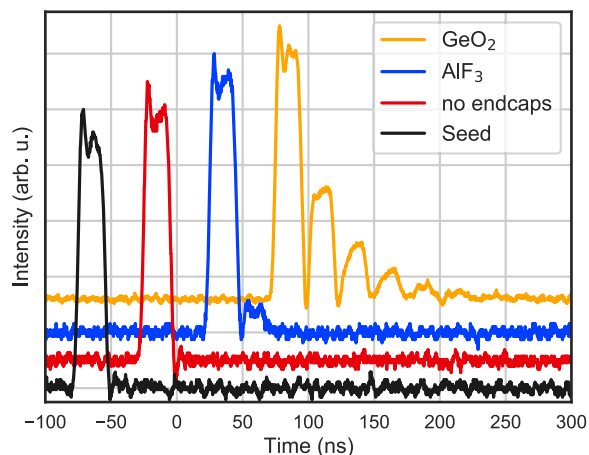


Fig. 7. Oscilloscope trace of the amplified output pulses at a repetition rate of 1 MHz and pulse duration of 20 ns for different end-cap configurations: input pulse shape (black), bare fibre ends (red),  $\text{AlF}_3$  end-caps on both ends (blue), and one  $\text{GeO}_2$  end-cap at the output facet (orange).

of 32 dB is obtained in the fibre section. This corresponds to a theoretical net-gain of  $-15.8$  dB over a full round-trip in the fibre amplifier, i.e. two Fresnel reflections at the end-caps and two passes through the fibre section, which would result in a satellite pulse with a relative energy of 2.6%. This theoretical estimate is in good qualitative agreement with the experimental results. However, detailed numerical modelling of the gain distribution along the fibre section will be required to obtain more accurate predictions of satellite pulse formation and predict the impact of back-reflections on amplification.

For the last amplifier configuration, with one  $\text{GeO}_2$  end-cap at the output end, a maximum output power of 58 mW was obtained at a pump power of 3.4 W. Further increase of the pump power resulted in self-lasing inside the fibre section. The achieved output power corresponds to an amplifier gain of 16 dB and an optical efficiency of only 1.7%. The oscilloscope trace shows a series of decreasing satellite pulses, which contain 44% of the total pulse energy. The low optical efficiency and the formation of satellite pulses can be directly linked to the large mismatch in refractive indexes between the fibre core and the  $\text{GeO}_2$  end-cap. The end-cap has a refractive index of 1.83, which results in a reflection of 1% ( $-10$  dB) at the interface with the fibre section. Thus, the single-pass gain in the fibre section (24 dB) is sufficient to compensate for back-reflection losses and amplify the back-propagating pulses. Even the bare angle-cleaved fibre end, with an estimated back-reflection loss of 45–50 dB, is not sufficient to suppress the build-up of satellite pulses. Furthermore, the back-reflection at the  $\text{GeO}_2$  end-cap leads to significant laser output in the back-propagating direction (not possible to measure in our setup), which reduces the optical efficiency in forward direction.

Only the fibre amplifier configuration with  $\text{AlF}_3$  end-caps provided stable laser performance throughout the experiments. A deterioration in laser performance was observed for the two other configurations after 1–2 hours of operation at the maximum output powers—attributed to degradation of the unprotected bare fibre facets [26].

## VI. CONCLUSION

We have presented the amplification of electrically-pumped GaSb-based diode lasers in an Er-doped fluoride fibre amplifier. While the fibre-based amplification of diode lasers is a common approach for laser development at wavelengths in the NIR, it is demonstrated here for the first time in the MIR at laser wavelengths around  $2.8 \mu\text{m}$ . Direct electrical control of the GaSb-based diode lasers enabled the investigation of different laser operation regimes and the flexible tuning of ns-pulse durations and repetition rates. The demonstrated laser parameters include: CW output powers up to 934 mW, amplification of ns-pulses with durations as short as 20 ns, pulse repetition rates up to 1 MHz, and pulse energies up to  $3.25 \mu\text{J}$ . Fibre amplifier gain values of up to 26 dB have been achieved, limited only by the onset of self-lasing in the fibre section.

The experiments have been performed with two different GaSb-based Fabry-Pérot diode lasers, to ensure reproducibility and to demonstrate that the proposed laser design can be implemented with currently available commercial diode lasers. Additionally, three different fibre end-cap configurations have been compared. The obtained results show that Fresnel reflections at end-cap interfaces have a significant impact on amplification and result in the emergence of satellite pulse at sufficiently high gain levels.

Apart from significantly extending the range of accessible laser parameters at wavelengths around  $2.8 \mu\text{m}$ , the demonstrated laser system represents an important proof-of-concept, which opens several possibilities for further laser development in the MIR. First, the presented laser setup can be further improved in terms of output power by more efficient seed laser coupling, increase of available pump power, and reduction of end-cap back-reflections, either through index-matching or novel end-cap designs. Furthermore, a large variety of GaSb-based diode lasers is available in the mid-infrared, e.g. VECSEL [28], tunable lasers [15], and mode-locked lasers [29], which can be integrated into the presented laser setup to obtain different laser characteristics. Other wavelength ranges in the MIR can also be accessed by replacement of the Er-doped fibre with other rare-earth doped fluoride fibres. Finally, the development of multi-stage fibre amplification systems [21], [22] holds significant potential for further power scaling.

## REFERENCES

- [1] L. A. Coldren, S. W. Corzine, and M. L. Mašanović, *Diode Lasers and Photonic Integrated Circuits*. Hoboken, NJ, USA: Wiley, 2012.
- [2] D. J. Richardson, J. Nilsson, and W. A. Clarkson, "High power fiber lasers: Current status and future perspectives [Invited]," *J. Opt. Soc. Amer. B.*, vol. 27, no. 11, pp. B63–B92, 2010.
- [3] W. Shi, Q. Fang, X. Zhu, R. A. Norwood, and N. Peyghambarian, "Fiber lasers and their applications [Invited]," *Appl. Opt.*, vol. 53, no. 28, pp. 6554–6568, 2014.
- [4] M. N. Zervas and C. A. Codemard, "High power fiber lasers: A review," *IEEE J. Sel. Topics Quantum Electron.*, vol. 20, no. 5, pp. 219–241, Sep/Oct. 2014.
- [5] G. P. Agrawal, *Fiber-Optic Communication Systems*, 5th ed. Hoboken, NJ, USA: Wiley, 2022.
- [6] N. Picqué and T. W. Hänsch, "Mid-IR spectroscopic sensing," *Opt. Photon. News*, vol. 30, no. 6, pp. 26–33, 2019.
- [7] S. De Bruyne, M. M. Speeckaert, and J. R. Delanghe, "Applications of mid-infrared spectroscopy in the clinical laboratory setting," *Crit. Rev. Clin. Lab. Sci.*, vol. 55, no. 1, pp. 1–20, 2018.
- [8] C. Frayssinous, V. Fortin, J.-P. Bérubé, A. Fraser, and R. Vallée, "Resonant polymer ablation using a compact  $3.44 \mu\text{m}$  fiber laser," *J. Mater. Process. Technol.*, vol. 252, pp. 813–820, 2018.
- [9] M. Skorczakowski et al., "Mid-infrared Q-switched Er:YAG laser for medical applications," *Laser Phys. Lett.*, vol. 7, no. 7, 2010, Art. no. 498.
- [10] M. C. Pierce, S. D. Jackson, M. R. Dickinson, T. A. King, and P. Sloan, "Laser-tissue interaction with a continuous wave  $3\text{-}\mu\text{m}$  fibre laser: Preliminary studies with soft tissue," *Lasers Surg. Med.*, vol. 26, no. 5, pp. 491–495, 2000.
- [11] P. Rechmann, D. S. Goldin, and T. Hennig, "Er: YAG Lasers in dentistry: An overview," *Proc. SPIE*, vol. 3248, pp. 2–13, 1998.
- [12] F. Nürnberg et al., "Bulk damage and absorption in fused silica due to high-power laser applications," *Proc. SPIE*, vol. 9632, pp. 354–363, 2015.
- [13] J. E. Bertie and Z. Lan, "Infrared intensities of liquids XX: The intensity of the OH stretching band of liquid water revisited, and the best current values of the optical constants of  $\text{H}_2\text{O}(l)$  at  $25^\circ\text{C}$  between 15,000 and  $1 \text{ cm}^{-1}$ ," *Appl. Spectrosc.*, vol. 50, no. 8, pp. 1047–1057, 1996.
- [14] L. Shterengas et al., "Cascade pumping of  $1.9\text{--}3.3 \mu\text{m}$  Type-I quantum well GaSb-based diode lasers," *IEEE J. Sel. Topics Quantum Electron.*, vol. 23, no. 6, pp. 1–8, Nov./Dec. 2017.
- [15] N. B. Chichkov et al., "Wavelength-tunable, GaSb-Based, cascaded Type-I quantum-well laser emitting over a range of  $300 \text{ nm}$ ," *IEEE Photon. Technol. Lett.*, vol. 30, no. 22, pp. 1941–1943, Nov. 2018.
- [16] S. D. Jackson, "Towards high-power mid-infrared emission from a fibre laser," *Nature Photon.*, vol. 6, no. 7, pp. 423–431, 2012.
- [17] S. D. Jackson and R. K. Jain, "Fiber-based sources of coherent MIR radiation: Key advances and future prospects (invited)," *Opt. Exp.*, vol. 28, no. 21, 2020, Art. no. 30964.
- [18] Y. O. Aydin, V. Fortin, R. Vallée, and M. Bernier, "Towards power scaling of  $28 \mu\text{m}$  fiber lasers," *Opt. Lett.*, vol. 43, no. 18, pp. 4542–4545, 2018.
- [19] S. Duval et al., "Watt-level fiber-based femtosecond laser source tunable from  $2.8$  to  $3.6 \mu\text{m}$ ," *Opt. Letters*, vol. 41, no. 22, pp. 5294–5297, 2016.
- [20] J.-C. Gauthier, V. Fortin, S. Duval, R. Vallée, and M. Bernier, "In-amplifier mid-infrared supercontinuum generation," *Opt. Lett.*, vol. 40, no. 22, pp. 5247–5250, 2015.
- [21] Y. O. Aydin, V. Fortin, D. Kraemer, A. Fraser, R. Vallée, and M. Bernier, "High-energy picosecond pulses from a  $2850 \text{ nm}$  fiber amplifier," *Opt. Lett.*, vol. 43, no. 12, pp. 2748–2751, 2018.
- [22] Y. O. Aydin et al., "Dual stage fiber amplifier operating near  $3 \mu\text{m}$  with millijoule-level, sub-ns pulses at  $5 \text{ W}$ ," *Opt. Lett.*, vol. 46, no. 18, pp. 4506–4509, 2021.
- [23] N. B. Chichkov et al., "Amplification of nanosecond pulses in a single-mode erbium-doped fluoride fibre amplifier," *IEEE Photon. Technol. Lett.*, vol. 35, no. 1, pp. 3–6, Jan. 2023.
- [24] P. Ray et al., "Wavelength-tuning of nanosecond pulses in Er-doped fluoride fibre amplifier," *IEEE Photon. J.*, vol. 14, no. 5, pp. 1–5, Oct. 2022, Art. no. 1553105.
- [25] W. Du, X. Xiao, Y. Cui, J. Nees, I. Jovanovic, and A. Galvanauskas, "Demonstration of  $067\text{-mJ}$  and  $10\text{-ns}$  high-energy pulses at  $2.72 \mu\text{m}$  from large core Er:ZBLAN fiber amplifiers," *Opt. Lett.*, vol. 45, no. 19, 2020, Art. no. 5538.
- [26] N. Caron, M. Bernier, D. Faucher, and R. Vallée, "Understanding the fiber tip thermal runaway present in  $3 \mu\text{m}$  fluoride glass fiber lasers," *Opt. Express*, vol. 20, no. 20, pp. 22188–22194, 2012.
- [27] Y. O. Aydin, F. Maes, V. Fortin, S. T. Bah, R. Vallée, and M. Bernier, "Endcapping of high-power  $3 \mu\text{m}$  fiber lasers," *Opt. Exp.*, vol. 27, no. 15, 2019, Art. no. 20659.
- [28] A. Andrejew, S. Sprengel, and M.-C. Amann, "GaSb-based vertical-cavity surface-emitting lasers with an emission wavelength at  $3 \mu\text{m}$ ," *Opt. Lett.*, vol. 41, no. 12, 2016, Art. no. 2799.
- [29] T. Feng, L. Shterengas, T. Hosoda, A. Belyanin, and G. Kipshidze, "Passive Mode-Locking of  $3.25 \mu\text{m}$  GaSb-Based Cascade Diode Lasers," *ACS Photonics*, vol. 5, no. 12, pp. 4978–4985, 2018.